Spontaneous reorientations of meta-atoms and electromagnetic spatial solitons in a liquid metacrystal

Alexander A. Zharov and Alexander A. Zharov, Jr.
Institute for Physics of Microstructures, Russian Academy of Sciences, Nizhny Novgorod, 603950 Russia
and N.I. Lobachevsky State University, Nizhny Novgorod, 603950 Russia

Nina A. Zharova*
Institute of Applied Physics, Russian Academy of Sciences, Nizhny Novgorod, 603950 Russia
(Received 9 April 2014; published 26 August 2014)

We show that transverse electromagnetic waves propagating along an external static electric field in liquid metacrystal (LMC) can provoke spontaneous rearrangement of elongated meta-atoms that changes the direction of the anisotropy axis of the LMC. This kind of instability may reorient the meta-atoms from the equilibrium state parallel to a static field to the state along a high-frequency field and back at the different threshold intensities of electromagnetic waves in such a way that bistability in the system takes place. Reorientation of meta-atoms causes a change in the effective refraction index of LMC that creates, in turn, the conditions for the formation of bright spatial solitons. Such spatial solitons are the self-consistent domains of redirected meta-atoms with trapped photons. We find that the instability thresholds as well as energy flux captured by the spatial soliton can be easily managed by variation of the static electric field applied to the LMC. We study the effects of soliton excitation and collisions via numerical simulations.

DOI: 10.1103/PhysRevE.90.023207 PACS number(s): 42.79.−e, 78.67.Pt

I. INTRODUCTION

Liquid metacrystals (LMCs), that is, resonant elongated particles suspended in a viscous medium (for example, liquid) in a static (dc) electric field, have recently been suggested [1] as a new type of resonant metamaterial. LMCs potentially possess a number of unique properties, such as, for example, high tunability and very strong nonlinearity, absent in natural materials as well as in most known metamaterials. These properties are caused by meta-atom reorientation under the action of both dc and high-frequency (HF) electric fields resulting in redirection of the optical axis of LMCs. Furthermore, the resonant response of meta-atoms enhances LMC tunability and nonlinearity, which are in no way the tunability and nonlinearity of media composing LMCs.

In fact, any new metamaterial expands the capability of electromagnetic radiation control, which makes them very attractive for further applications. Indeed, in the past decade, a lot of different kinds of metamaterials have appeared, operating in frequency ranges from microwaves up to visible light. These include negative index linear and nonlinear metamaterials [2–9], plasmonic metamaterials [10–13], tunable and elastic metamaterials with controllable electromagnetic properties [14,15], different nanoparticle arrays [16,17], etc., which paved the way for achieving superresolution [18–20], subwavelength light localization [21–24], nanolasing [25–27], cloaking [28,29], and artificial mimicry coatings [30]. In this respect, LMCs might also find their niche among other metamaterials, and a comprehensive study of their electromagnetic potentiality in different frequency domains seems to be highly important.

In this paper, we show that transverse electromagnetic waves propagating along a dc electric field in LMC can trigger an instability leading to meta-atom reorientation and consequently to the changing of the effective refraction index of the metamaterial. In the frequency range where the effective refraction index increases due to the meta-atom re-orientation, the conditions of the photon confinement in the self-consistent waveguide channels (spatial solitons) arise. One should notice that a nonlinear change of refractive index at frequencies close to resonance can be of the same order, greater than, or even much greater than its unperturbed value, which, according to the terminology accepted in the optics of conventional liquid crystals [31,32], corresponds to colossal or maybe supercolossal nonlinearity.

II. ELECTROMAGNETIC WAVES IN LMC: SIMPLIFIED MODEL

For further analysis, we keep the model used in our recent paper [1] of resonant dumbbell-like elongated metal subwavelength particles (meta-atoms) suspended in viscous liquid. The chosen specific shape of meta-atoms shown in Fig. 1 just allows us to determine its resonant frequency and quality factor in the simplest way, bearing in mind that dumbbell spheres define the capacitance of a meta-atom, $C = \varepsilon_l a$, while the straight dumbbell handle determines the inductance $L = 2lL_W$ and resistance $R = 2\rho l/\pi r^2$ (the ESU is used throughout the paper), where a is the radius of the dumbbell sphere, ε_l is the dielectric permittivity of surrounding liquid, $2l$ is the length of the dumbbell handle, $L_W = \frac{2}{c^2}\log\frac{d}{r}$ is the inductance per unit length of the direct wire of circular section [33], ρ is the specific resistance of the metal, r is the radius of the handle, $d = \min\{2l; N^{-1/3}; \lambda_l\}$ is some characteristic distance truncating logarithmic divergence of the inductance of the straight wire, N is the volume density of meta-atoms, $\lambda_l = 2\pi c/\omega\sqrt{\varepsilon_l}$ is the electromagnetic wavelength in surrounding liquid, and c is the speed of light.

*zhani@appl.sci-nnov.ru

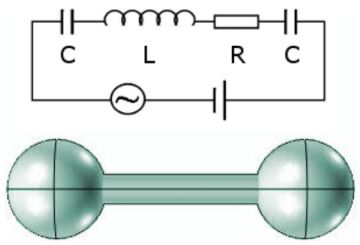

FIG. 1. (Color online) Schematic view of a meta-atom and an equivalent electric circuit (inset).

It is necessary to note that the considered model of dumbbell-like meta-atoms has a certain generality because it gives qualitatively identical results for any resonant elongated subwavelength meta-atoms, which enables us to avoid quite complicated simulations, at least in the first step of LMC study. The tensor of effective dielectric permittivity of the LMC with identically aligned meta-atoms has the form [1]

$$\hat{\varepsilon}_{\rm eff} = \varepsilon_l + 4\pi\,\chi_m(\omega)\hat{\sigma}, \tag{1}$$

where

$$\chi_m(\omega) = \frac{3}{4\pi}\,\frac{\omega_C^2}{\omega_s^2 - \omega^2 + i\gamma\omega}, \tag{2}$$

$$\hat{\sigma} = \begin{pmatrix} \cos^2\phi\sin^2\theta & \sin\phi\cos\phi\sin^2\theta & \cos\phi\sin\theta\cos\theta \\ \sin\phi\cos\phi\sin^2\theta & \sin^2\phi\sin^2\theta & \sin\phi\sin\theta\cos\theta \\ \cos\phi\sin\theta\cos\theta & \sin\phi\sin\theta\cos\theta & \cos^2\theta \end{pmatrix}, \tag{3}$$

$\omega_s^2 = \omega_0^2 - \omega_C^2$, $\omega_0 = 1/\sqrt{LC}$ is the resonant frequency of the meta-atom, $\omega_C^2 = 4\pi l N c^2/3\log(d/r)$ is the so called Lorenz shift of resonant frequency in the array of interacting oscillators [33], and $\gamma = R/L$. Expressions (1)–(3) describe effective uniaxial crystal with the axis characterized by spherical angles ϕ and θ or, in the same way, by the unit vector $\mathbf{e}_0$ with Cartesian components $(\mathbf{e}_0)_x = \cos\phi\sin\theta$, $(\mathbf{e}_0)_y = \sin\phi\sin\theta$, $(\mathbf{e}_0)_z = \cos\theta$, which is called the director. The direction of the optical axis of LMC is determined by the director, and it can be changed under the influence of both dc and HF electric fields. The dynamics of meta-atoms with two active rotational degrees of freedom obeys the following equations, written in terms of spherical angles ϕ and θ [1]:

$$\frac{d^2\theta}{dt^2} - \left(\frac{d\phi}{dt}\right)^2 \sin\theta\cos\theta + \xi\frac{d\theta}{dt} = A_0 q(E_x\cos\phi\cos\theta + E_y\sin\phi\cos\theta - E_z\sin\theta), \tag{4}$$

$$\frac{d}{dt}\left(\frac{d\phi}{dt}\sin^2\theta\right) + \xi\frac{d\phi}{dt}\sin^2\theta = -A_0 q\sin\theta(E_x\sin\phi - E_y\cos\phi), \tag{5}$$

$$\frac{d^2q}{dt^2} + \gamma\frac{dq}{dt} + \omega_s^2 q = B_0(E_x\cos\phi\sin\theta + E_y\sin\phi\sin\theta + E_z\cos\theta), \tag{6}$$

where $E_{x,y,z}$ are the Cartesian components of a macroscopic electric field (including both dc and HF fields) acting on a meta-atom, q is the charge induced by an external electric field in the meta-atom, $A_0 = 3/(4\pi\eta_\Sigma a^3 l)$, $B_0 = c^2/[2\log(d/r)]$, $\xi = 3\nu/(4\pi\eta_\Sigma a^3)$, ν is the kinematic viscosity, and η_Σ is the density of meta-atom material, including correction because of the added mass of the liquid. Within the framework of quasistationary interaction of an electromagnetic field with LMC, a self-consistent director orientation can be found, assuming that the right-hand parts of Eqs. (4) and (5) averaged over the period of the HF electromagnetic field are equal to zero,

$$R^{(\theta)} \equiv \langle q(t)[E_x(t)\cos\phi\cos\theta + E_y(t)\sin\phi\cos\theta - E_z(t)\sin\theta]\rangle_t = 0, \tag{7}$$

$$R^{(\phi)} \equiv \langle q(t)\sin\theta[E_x(t)\sin\phi - E_y(t)\cos\phi]\rangle_t = 0, \tag{8}$$

where the angular brackets denote the corresponding averaging procedure.

III. INSTABILITY AND BISTABILITY OF LMC IN THE FIELD OF A STRONG ELECTROMAGNETIC WAVE

We consider a plane transverse electromagnetic wave propagating along an LMC polarization axis (say the z axis, $\mathbf{k} \parallel \mathbf{z}_0$, where $\mathbf{z}_0$ is the unit vector along z axis) which is assigned by the direction of the dc electric field $\mathbf{E}_0 = E_0\mathbf{z}_0$. The linear polarization of the wave is assumed to be directed along the x axis: $\mathbf{E} \parallel \mathbf{x}_0$, $\mathbf{x}_0$ is the corresponding unit vector. The HF field of the electromagnetic wave has zero projection upon the dc field direction, so elongated meta-atoms do not affect the propagation conditions, and the wave travels as in a medium with dielectric permittivity ε_l. However, such a stationary regime takes place only up to some critical intensity of the wave, $I = |\mathbf{E}|^2 < I_c$. If the intensity exceeds this threshold value, the state with $\mathbf{k} \parallel \mathbf{e}_0 \perp \mathbf{E}$ becomes unstable. To obtain a stability criterion, one should linearize Eq. (4) with the right-hand part time-averaged over the period of the HF field (taking into account that the mechanical motion is much slower in comparison with the HF field) in the vicinity of $\theta \sim 0$. In this case, ϕ is a degenerate variable and it can be considered as an arbitrary constant value; $\phi = \text{const}$. A new component of electric field E_z that arose due to a deflection of meta-atom axes from the equilibrium state $\theta = 0$ can be found from the condition of the zero longitudinal component of the electric displacement, $D_z = (\hat{\varepsilon}_{\rm eff}\mathbf{E})_z = 0$,

$$E_z = -\frac{\Delta\varepsilon\sin\theta\cos\theta\cos\phi}{\varepsilon_l + \Delta\varepsilon\cos^2\theta}E_x, \tag{9}$$

where $\Delta\varepsilon = 4\pi\chi_m(\omega)$. It is easy to show that the E_y component of the electric field emerging at $\phi \neq 0$ is of the second order of smallness $E_y \sim \theta^2$ at $\theta \ll 1$ and, therefore, it should not be taken into account. As a result, we come to the equation describing the dynamics of a meta-atom in the vicinity of equilibrium state $\theta = 0$,

$$\frac{d^2\theta}{dt^2} + \xi\frac{d\theta}{dt} = R^{(\theta)} = \frac{A_0 B_0}{\omega_s^2}E_0^2\left\{-1 + 2\sigma_{\rm NL}^2\,{\rm Re}\left(\frac{\varepsilon_l F(\omega)}{\varepsilon_l + \Delta\varepsilon}\right)\cos^2\phi\right\}\theta, \tag{10}$$

where $\sigma_{\rm NL}^2 = |E_x|^2/E_0^2$, $F(\omega) = \omega_s^2/(\omega_s^2 - \omega^2 + i\gamma\omega)$. The ratio of the HF field amplitude to the static field strength ($\sigma_{\rm NL}$) plays the role of a nonlinear parameter. The equilibrium state with $\theta = 0$ becomes unstable when the value in the curly brackets on the right-hand side of Eq. (10) is positive, which in turn defines the stability threshold depending on frequency. One can see from Eq. (10) that a minimal threshold takes place at $\phi = 0$, implying the meta-atom rotation in the plane made up by vectors of dc and HF electric fields. This dynamics of meta-atoms somewhat resembles the so called Kapitza pendulum with an oscillating hanger point [34]. Most simply, the instability threshold can be calculated for a lossless medium with $\gamma = 0$. In this case, taking into account that $\Delta\varepsilon = \varepsilon_l\eta F(\omega)$ and $\eta = 3\omega_C^2/(\varepsilon_l\omega_s^2)$, we come to the desired stability criterion

$$\sigma_{\rm NL}^2 > \sigma_{C1}^2 \equiv \frac{1}{2}\left(\frac{1}{F(\omega)} + \eta\right), \quad \omega < \omega_s\sqrt{1+\eta}, \tag{11}$$

where $\sigma_{C1} = \sigma_C(\theta = 0)$ denotes the critical value of the nonlinear parameter calculated for $\theta = 0$.

Since we consider the mechanical rotations of meta-atoms as much slower in comparison with the oscillations of an electromagnetic field, formula (11) is valid down to lowest frequencies for which the averaging procedure on the right-hand part of Eq. (10) is still correct. The value $\Delta\varepsilon$ is positive at $\omega < \omega_s$ and $\omega > \omega_s\sqrt{1+\eta}$, which corresponds to the focusing nonlinearity of LMC, and $\Delta\varepsilon$ is negative at $\omega_s < \omega < \omega_s\sqrt{1+\eta}$, exhibiting defocusing nonlinearity of LMC. In a lossless case, the expression (11) gives a zero value of σ_C at the upper boundary of the frequency range, which indicates an infinite growing of the E_z component of the HF electric field due to excitation of the plasmalike longitudinal potential mode with $[\hat{\varepsilon}_{\rm eff}(\omega = \omega_s\sqrt{1+\eta})]_{zz} = 0$. More rigorous calculations for $\gamma \neq 0$ show that the instability disappears when $\omega > \omega_s\sqrt{1+\eta}$. The instability growth rate g can be found from Eq. (10). Writing $R^{(\theta)} = \omega_B^2(\sigma_{\rm NL},\omega)\theta$, we get

$$g = -\frac{\xi}{2} \pm \sqrt{\frac{\xi^2}{4} - \omega_B^2}. \tag{12}$$

As soon as ω_B^2 becomes negative, instability develops. Now we shall demonstrate that this instability leads to the meta-atom turnover that aligns them along the $\theta = \pi/2$, $\phi = 0$ direction, i.e., along the HF field. For that, one should find all equilibrium states and determine their stability at $\phi = 0$ and $E_y = 0$ within the framework of a lossless case, as before. Omitting obvious calculations, we adduce the final equation, which determines the equilibrium states in the system,

$$\sin\theta\cos\theta\left\{-1 + 2F(\omega)\sigma_{\rm NL}^2\left(1 - \frac{(\Delta\varepsilon)^2\sin^2\theta\cos^2\theta}{(\varepsilon_l + \Delta\varepsilon\cos^2\theta)^2} - \frac{\Delta\varepsilon(\cos^2\theta - \sin^2\theta)}{\varepsilon_l + \Delta\varepsilon\cos^2\theta}\right)\right\} = 0. \tag{13}$$

One can see that meta-atom orientations with $\theta = 0$ and $\theta = \pi/2$ are always equilibrium. We have already obtained the stability criterion for the equilibrium state $\theta = 0$. Carrying out calculations similar to those done for $\theta = 0$, one can find another critical nonlinear parameter σ_{C2}: For $\sigma_{\rm NL}$ exceeding this critical value,

$$\sigma_{\rm NL}^2 > \sigma_{C2}^2 \equiv \frac{1}{2F(\omega)[1 + \eta F(\omega)]}, \tag{14}$$

the equilibrium state $\theta = \pi/2$ becomes stable. The characteristic behavior of both critical nonlinear parameters along with $\Delta\varepsilon$ are shown in Fig. 2(a) as functions of the normalized frequency. In calculations, the following set of parameters was used: $l = 2\times10^{-4}$ cm, $a = 10^{-4}$ cm, $d = 10^{-3}$ cm, $r = 5\times10^{-5}$ cm, $N = 10^7$ cm^{-3}; the meta-atom material is silver with $\eta_\Sigma \approx 10{\rm g}\times{\rm cm}^{-3}$, $\varepsilon_l = 2$. It gives the values for the resonant frequency $\omega_0 \approx \omega_s \approx 6.1\times10^{13}$ s^{-1}, the damping coefficient $\gamma \approx 10^{-3}\times\omega_0 \approx 6.1\times10^{10}$ s^{-1}, the Lorentz shift frequency $\omega_C \approx 1.6\times10^{12}$ s^{-1}, and the parameter $\eta \approx 0.001$.

It is important that

$$\frac{\sigma_{C2}^2}{\sigma_{C1}^2} = \frac{1}{[1 + \eta F(\omega)]^2} < 1$$

for $F(\omega) > 0$, i.e., for $\omega < \omega_s$. Besides the orientations with $\theta = 0$ and $\theta = \pi/2$, an additional equilibrium state emerges that can be found from the solution of Eq. (13). As a result, we come to the explicit expression for new equilibrium, $\theta = \bar{\theta}$,

$$\cos^2\bar{\theta} = \frac{\sigma_{\rm NL}\sqrt{2\varepsilon_l F(\omega)(\varepsilon_l + \Delta\varepsilon)} - \varepsilon_l}{\Delta\varepsilon}. \tag{15}$$

This equilibrium state exists exactly within the intensity domain

$$\sigma_{C2}^2 < \sigma_{\rm NL}^2 < \sigma_{C1}^2, \tag{16}$$

as it immediately follows from expression (15) and it is unstable. Therefore, the three equilibrium states take place within this interval of electromagnetic wave intensity, two of them are stable ($\theta = 0$ and $\theta = \pi/2$), being of the stable focus type. The intermediate equilibrium state given by expression (15) is unstable, representing a saddle point. Thus, LMC turn out to be bistable in the intensity region (16) so that at the same value of the wave intensity, both stable orientations of the director are possible. The transition of LMC to one or another stable state depends on the temporal prehistory of the process. Therefore, in the increasing HF field, the meta-atoms transit from $\theta = 0$ to $\theta = \pi/2$ at $\sigma_{\rm NL}^2 > \sigma_{C1}^2$; when the field decreases, the transition occurs in the opposite direction at a smaller level of intensity, $\sigma_{\rm NL}^2 < \sigma_{C2}^2$. This hysteresis behavior is illustrated in Fig. 2(b). The model parameters $\Delta\varepsilon = 0.1 - 0.005i$, $\sigma_{C1}^2 = 0.0105$, and $\sigma_{C2}^2 = 0.0095$ used in the calculations of this dependence were obtained for $\omega = 0.99\omega_s$. The factor η is small in the case of quite rare

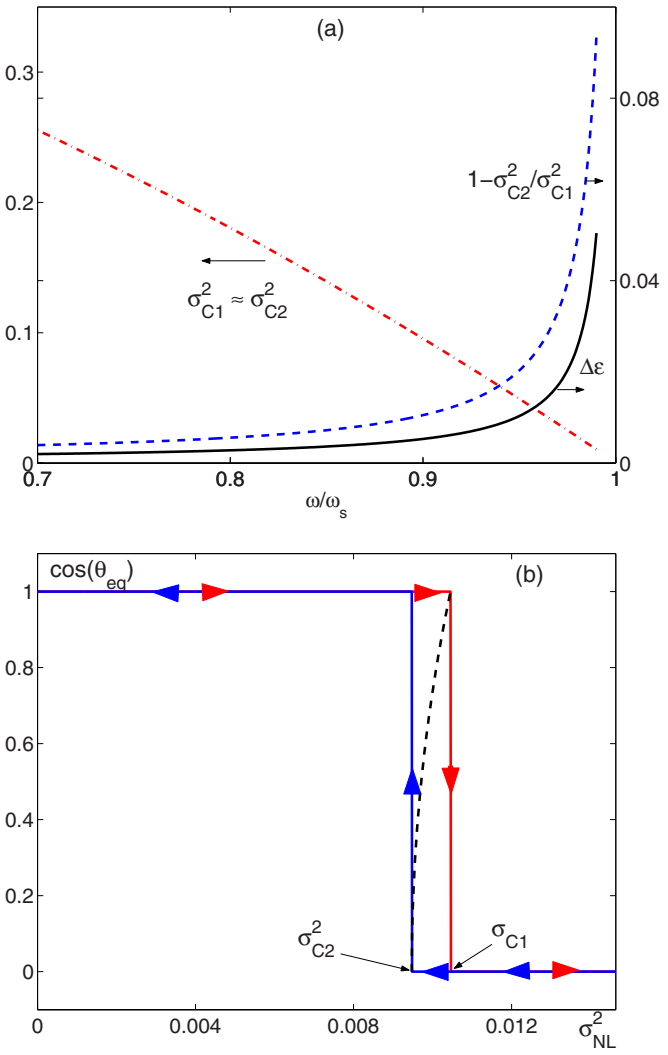

FIG. 2. (Color online) (a) Dependence of the critical values of the nonlinear parameter $\sigma_{C1}^2 \approx \sigma_{C2}^2$ (left axis, dash-dotted line) and also their normalized difference, $1 - \sigma_{C2}^2/\sigma_{C1}^2$, and $\Delta\varepsilon$ (right axis, dashed and solid lines, respectively) on the normalized frequency ω/ω_s. (b) Cosine of the equilibrium orientation angle as a function of nonlinearity parameter $\sigma_{\rm NL}^2$: When the HF field increases, the switching from $\theta_{\rm eq} = 0$ to $\theta_{\rm eq} = \pi/2$ takes place at $\sigma_{\rm NL} = \sigma_{C1}$; a decreasing field induces the inverse switch at lower $\sigma_{\rm NL} = \sigma_{C2}$. The dashed line shows the behavior of unstable $\theta_{\rm eq} = \bar{\theta}$ [see Eq. (15)]. The hysteresis behavior becomes clear in the vicinity of resonance (in the calculations, $\omega = 0.99\omega_s$ was used). If this is not the case, the critical fields for "on" and "off" switching are quite close to each other.

meta-atom suspension, and thus the difference between the two critical nonlinear parameters is $\delta\sigma_C^2 \equiv \sigma_C^2(\theta = 0) - \sigma_C^2(\theta = \pi/2) \ll 1$. For any $\omega < \omega_s$ not too close to resonance, this difference $\delta\sigma_C^2 \approx \eta$, and approaching the resonance, $\delta\sigma_C^2 \to 0$. However, in the vicinity of resonance, $\sigma_C^2(\theta = 0)$ also tends to zero, the normalized difference $\delta\sigma_C^2/\sigma_C^2(\theta = 0)$ increases, and the hysteresis becomes more pronounced at $\omega/\omega_s \approx 1$. The reorientation of meta-atoms in the frequency domain $\omega < \omega_s$ leads to the switching of effective dielectric permittivity in such a way that in a stronger (superthreshold) field, the refraction index is larger than in a smaller (subthreshold) field. This means that in a transversally inhomogeneous wave field, for example in an electromagnetic beam, a spatial domain can arise with a higher refraction index, which provides conditions for the field localization. The width of such a domain in the stationary case is determined self-consistently, taking into account that the HF field intensity at the domain walls is equal to the threshold value. In the case of defocusing nonlinearity, a similar stepwise permittivity structure resides in the frequency domain $\omega_s < \omega < \omega_s\sqrt{1+\eta/2}$. However, for higher frequency ($\omega_s\sqrt{1+\eta/2} < \omega < \omega_s\sqrt{1+\eta}$), where $\Delta\varepsilon$ is still negative, both states $\theta = 0$ and $\theta = \pi/2$ become unstable, and the meta-atoms take some intermediate orientation depending on the local field intensity $I(y,z)$: $0 < \theta(I) < \pi/2$.

IV. BRIGHT SPATIAL SOLITONS

The presence of the domain of identically reoriented meta-atoms with higher refractive index makes it possible to confine the electromagnetic radiation inside the domain, or, in other words, to form an electromagnetic spatial soliton. Actually, the bright spatial soliton in LMC is the self-consistent fundamental mode of TE-type of a planar waveguide in which the effective dielectric permittivity is $\varepsilon_{\rm eff}^{\rm (in)} = \varepsilon_l + \Delta\varepsilon$ inside the waveguide and $\varepsilon_{\rm eff}^{\rm (out)} = \varepsilon_l$ outside. It is caused by the absence of off-diagonal components of the tensor of effective dielectric permittivity when the director orients along the z or x axes while the HF electric field in the wave propagating along the bias direction z has a sole component E_x. In the stationary case, Maxwell's equations yield the expression for $E_x(y)$ in a localized nonlinear mode,

$$\frac{d^2E_x}{dy^2} + \left[k_0^2\varepsilon_{\rm eff}(|E_x|^2) - k^2\right]E_x = 0, \tag{17}$$

where

$$\varepsilon_{\rm eff}(|E_x|^2) = \varepsilon_l, \quad |E_x|^2 < E_C^2 \tag{18}$$

for the case of meta-atoms aligned along the dc field, and

$$\varepsilon_{\rm eff}(|E_x|^2) = \varepsilon_l + \Delta\varepsilon, \quad |E_x|^2 > E_C^2 \tag{19}$$

if the meta-atoms are aligned along the HF electric field; E_C is one of the instability threshold fields on the boundaries of the bistability zone. We assume that the electromagnetic wave is traveling along $z \sim \exp(-ikz)$. The boundary conditions at the domain walls in the plane (x,z) correspond to the continuity of tangential components of electric (E_x) and magnetic $[H_z = (ik_0)^{-1}dE_x/dy]$ fields. Furthermore, the HF electric-field amplitude at the domain walls has to be equal to that of the instability threshold values, which correspond either to σ_{C1} or σ_{C2}, which are the same at both walls. One can show that only single-hump spatial solitons are realized, and neither multihump (except periodic) nor asymmetric solutions may exist because it is impossible to satisfy the foregoing boundary conditions. The domain width a of the meta-atoms reoriented in an alternative electric field is to be determined self-consistently. The transverse field structure of the spatial soliton can be found by solving Eq. (17), taking into account boundary conditions. According to Eq. (17), the electric field inside and outside the reoriented-meta-atom domain can be

written as follows:

$$E_x = E_m \cos(\kappa_{\rm in} y), \quad |y| < b/2, \tag{20}$$

$$E_x = E_C \exp[-\kappa_{\rm out}(|y| - b/2)], \quad |y| \geqslant b/2 \tag{21}$$

where $\kappa_{\rm in} = \sqrt{k_0^2(\varepsilon_l + \Delta\varepsilon) - k^2}$, $\kappa_{\rm out} = \sqrt{k^2 - k_0^2\varepsilon_l}$, b is the width of the domain, and E_m is the electric field amplitude at the soliton peak. Then, tailoring E_x and dE_x/dy at $y = \pm b/2$, we come to the nonlinear dispersion equation for the spatial soliton along with formulas describing its peak amplitude E_m and domain width b via wave number k:

$$(E_C/E_m)^2 \equiv \beta^2 = \left(1 + \kappa_{\rm out}^2/\kappa_{\rm in}^2\right)^{-1}, \tag{22}$$

$$\tan(\kappa_{\rm in} b/2) = \sqrt{1 - \beta^2}/\beta, \tag{23}$$

$$\kappa_{\rm in}\tan(\kappa_{\rm in} b/2) = \kappa_{\rm out}. \tag{24}$$

Only two expressions from Eqs. (22)–(24) are independent, and a third one is their consequence. Thus, we can fix any one of the parameters, and the other two may be obtained through this given value. One of the important characteristics of the spatial soliton is a total energy flux per unit length along x,

$$P = \int_{-\infty}^{\infty} S_z(y)dt, \tag{25}$$

where $S_z = c\,{\rm Re}(E_x H_y^*)/(8\pi) = ck|E_x|^2/(8\pi k_0)$ is the time-averaged density of energy flux. The integration of Eq. (25) leads to the expression for the total energy flux,

$$P(k) = \frac{kcE_C^2}{8\pi k_0 \kappa_{\rm out}} \left\{1 + \alpha(1+\alpha^2){\rm arctan}\left(\frac{\alpha}{1+\alpha^2}\right) + \alpha^2\right\}, \tag{26}$$

where $\alpha = \kappa_{\rm out}/\kappa_{\rm in}$. In Fig. 3, the dependencies of $P(\delta k/k_0)/P_0$ ($P_0 = cE_0^2/8\pi k_0$), $k_0 b(\delta k/k_0)$, and $\beta(\delta k/k_0)$ ($\delta k/k_0 = k/k_0 - \sqrt{\varepsilon_l}$) for different frequencies are shown in (a), (b), and (c), respectively. One can see that the dependence $P(k)$ has a minimum and tends to infinity in the vicinity of the verges of the soliton existence domain: $k_0^2\varepsilon_l < k^2 < k_0^2(\varepsilon_l + \Delta\varepsilon)$. At the lower verge, $k \to k_0\sqrt{\varepsilon_l}$, the soliton field is weakly localized outside of the reoriented meta-atom domain and the localization disappears completely exactly at the verge and $b \to 0$, $\beta \to 1$ ($E_m \to E_C$). At the upper verge, $k \to k_0\sqrt{\varepsilon_l + \Delta\varepsilon}$, all the energy flux is actually concentrated inside the domain of reoriented meta-atoms so that $\beta \to 0$ ($E_m \to \infty$), and $b \approx \pi/\kappa_{\rm in} \to \infty$ as follows from expressions (22) and (23). According to the Vakhitov-Kolokolov criterion [35,36], the spatial bright solitons are stable if $dP/dk > 0$, and they are unstable in the opposite case when $dP/dk < 0$. Thus, only the growing branch of the curve $P(k)$ is stable when $k_{\rm min} < k < k_0\sqrt{\varepsilon_l + \Delta\varepsilon}$, where $k_{\rm min}$ corresponds to the wave number for which $dP/dk = 0$. Therefore, to excite the spatial soliton by external radiation, for example by a wave beam, the required total energy flux must be at least greater than $P_{\rm min}$; $P_{\rm beam} > P_{\rm min} = P(k_{\rm min})$. This is illustrated in Fig. 4, where the results of numerical simulations of the soliton excitation in LMC by an electromagnetic beam in both subcritical $P_{\rm beam} < P_{\rm min}$ [Fig. 4(a)] and supercritical $P_{\rm beam} > P_{\rm min}$ [Fig. 4(b)] regimes are shown. In the first case, the beam scatters without soliton formation, whereas

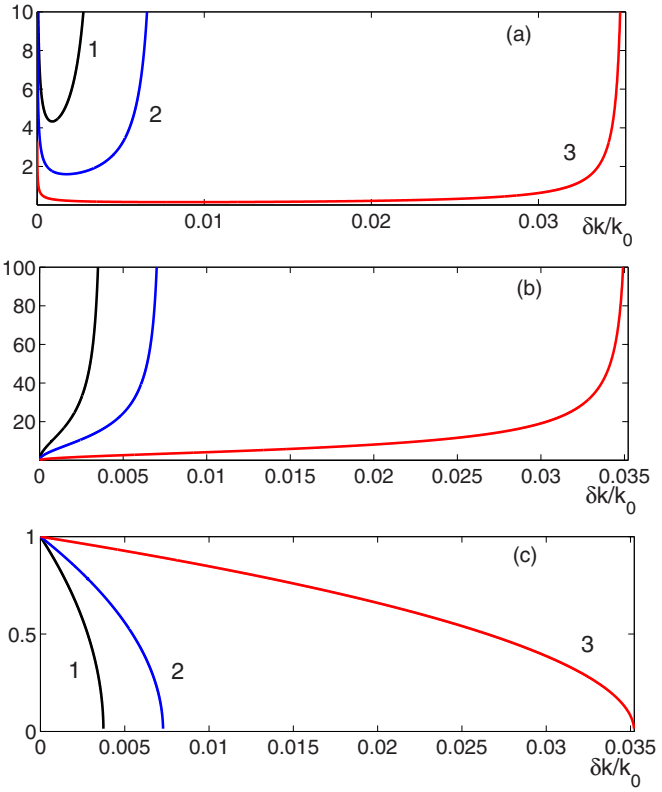

FIG. 3. (Color online) Dependence of the bright soliton parameters P/P_0 (a), $k_0 b$ (b), and β (c) as functions of $\delta k/k_0 \equiv k/k_0 - \sqrt{\varepsilon_l}$. Curves (1), (2), and (3) correspond to $\omega/\omega_s = 0.9$, 0.95, and 0.99.

in the supercritical case the beam field is captured into a self-consistent wave channel, as shown in Fig. 4(c). These and further simulations have been carried out within the framework of the nonlinear Schrödinger equation,

$$-2ik_0\sqrt{\varepsilon_l}\frac{\partial\psi}{\partial z} + \frac{\partial^2\psi}{\partial y^2} + k_0^2[\varepsilon_{\rm eff}(|\psi|^2) - \varepsilon_l]\psi = 0, \tag{27}$$

where $E_x = \psi(z,y)\exp(-ik_0\sqrt{\varepsilon_l}z)$, $\psi(z,y)$ is the HF electric-field amplitude considered as a slowly varying function of z, and $\varepsilon_{\rm eff}(|\psi|^2)$ is given by Eqs. (18) and (19). The initial transverse field structure is specified at $z = 0$. Figure 5 demonstrates the interaction and collision of two converging spatial solitons in LMC excited by two displaced Gaussian in-phase beams. Figure 5(a) illustrates the linear process of dispersion spread of narrow initial beams, and in Fig. 5(b) the nonlinear interaction of these two beams is shown. In-phase spatial solitons attract each other, and since Eq. (25) belongs to the nonintegrable class, its solutions allow inelastic soliton collisions, which only occur as a result of joining the reoriented meta-atom domains [see Fig. 5(c)]. It should be noted that joining the two beams together is accompanied by considerable radiation loss of the initial energy flux, however the amplitude $A_0 = 1.5$ is sufficient for the emergence of the soliton-type solution.

In Fig. 6, the interaction of repulsive out-of-phase beams is shown. Comparing again linear [Fig. 6(a)] and nonlinear [Figs. 6(b) and 6(c)] regimes, one can see that in this case for the field distribution with the amplitude $A_0 = 1.5$, the

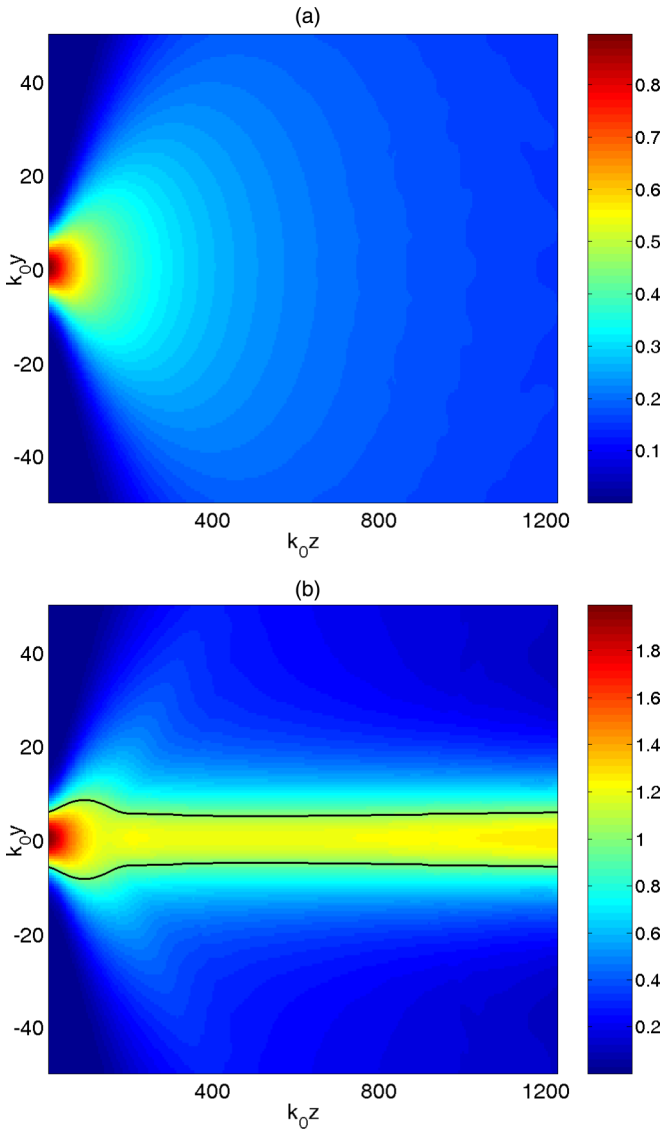

FIG. 4. (Color online) Spatial structure of normalized field $|E/E_c|$ in the case of subcritical (a) and supercritical (b) amplitude; the solid line shows the boundaries of the reoriented meta-atom domain. The field amplitude at $z = 0$ is taken in the form of a Gaussian beam, $E/E_c = A_0 \exp[-(y)^2/2w^2]$, with $k_0 w = 5$, $A_0 = 0.9$, and $A_0 = 2$ for the subcritical and supercritical structures, respectively; $\omega/\omega_s = 0.95$.

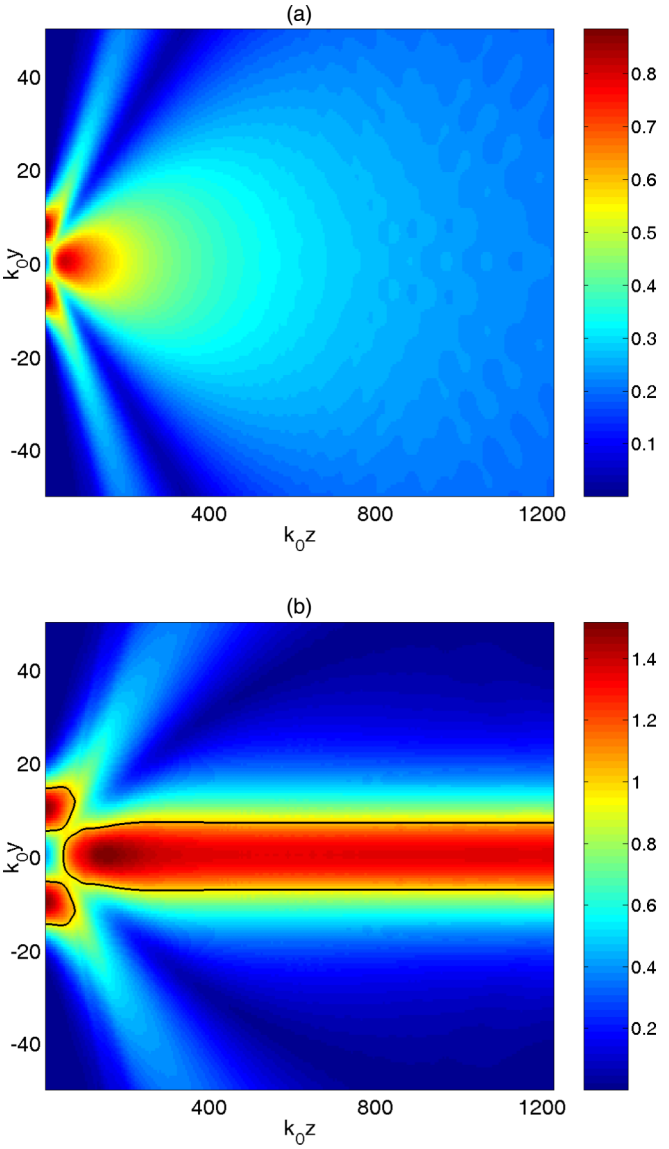

FIG. 5. (Color online) Spatial structure of normalized field $|E/E_c|$ in the case of subcritical (a) and supercritical (b) amplitude; the solid line shows the boundaries of the reoriented meta-atom domain. The field amplitude at $z = 0$ is taken in the form of two in-phase Gaussian beams $E/E_c = A_0\{\exp[-(y/w - h)^2/2] + \exp[-(y/w + h)^2/2]\}$ with $h = 2$; $k_0 w = 5$; $A_0 = 0.9$ and 1.5 for the subcritical and supercritical structures, respectively; and $\omega/\omega_s = 0.95$.

reoriented meta-atom domain (the domain boundaries are shown by the contour line) is formed only at the initial part of the beams paths, and after that the field evolution in Fig. 6(b) becomes linear. However, formation of solitons could be achieved for higher amplitude. This case is illustrated in Fig. 6(c), where the two divergent solitons form. This non-interacting propagation takes place because upon increasing the distance between the solitons, the field overlap decreases exponentially.

The initial distributions for in-phase (Fig. 5) and out-of-phase (Fig. 6) fields are very similar. These both functions are a sum of two Gaussian beams $E/E_c = A_1 \exp[-(y/w_1 - h)^2/2 + i\phi_1] + A_2 \exp[-(y/w_2 + h)^2/2 + i\phi_2]$ with equal amplitudes $A_1 = A_2$ and widths $w_1 = w_2$, and differ only by the phase shift $\Delta\phi = \phi_2 - \phi_1$ between them ($\Delta\phi = 0$ and $\Delta\phi = \pi$). So it is interesting to look at the intermediate case with $\Delta\phi = \pi/2$. The corresponding field evolution is illustrated in Fig. 7 for subcritical as well as supercritical regimes. The obtained supercritical spatial dynamics of the soliton channel maintains the features of both in-phase and out-of-phase solutions. The two input beams produce two domains of reoriented meta-atoms generating eventually a sole soliton channel with a direction slightly deviated from the z axis.

The energy flux captured by the spatial soliton is proportional to the critical field E_C, which in turn is proportional to the dc electric field E_0. Hence, this energy flux along with

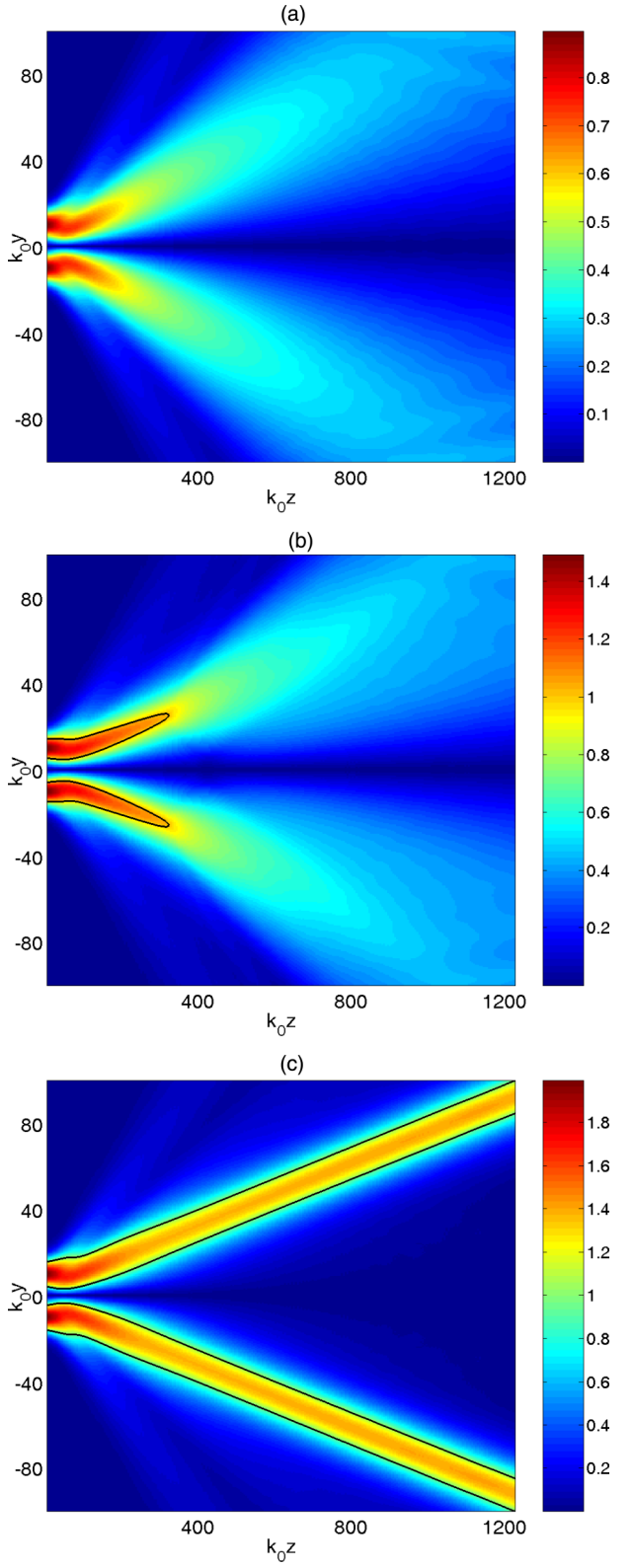

FIG. 6. (Color online) Spatial structure of normalized field $|E/E_c|$ in the case of subcritical (a), intermediate (b), and supercritical (c) amplitude; the solid line shows the boundaries of the reoriented meta-atom domain. The field amplitude at $z = 0$ is taken in the form of two out-of-phase Gaussian beams $E/E_c = A_0\{\exp[-(y/w - h)^2/2] - \exp[-(y/w + h)^2/2]\}$ with $h = 2$; $k_0 w = 5$; $A_0 = 0.9$, 1.5, and 2 for cases (a), (b), and (c), respectively; and $\omega/\omega_s = 0.95$.

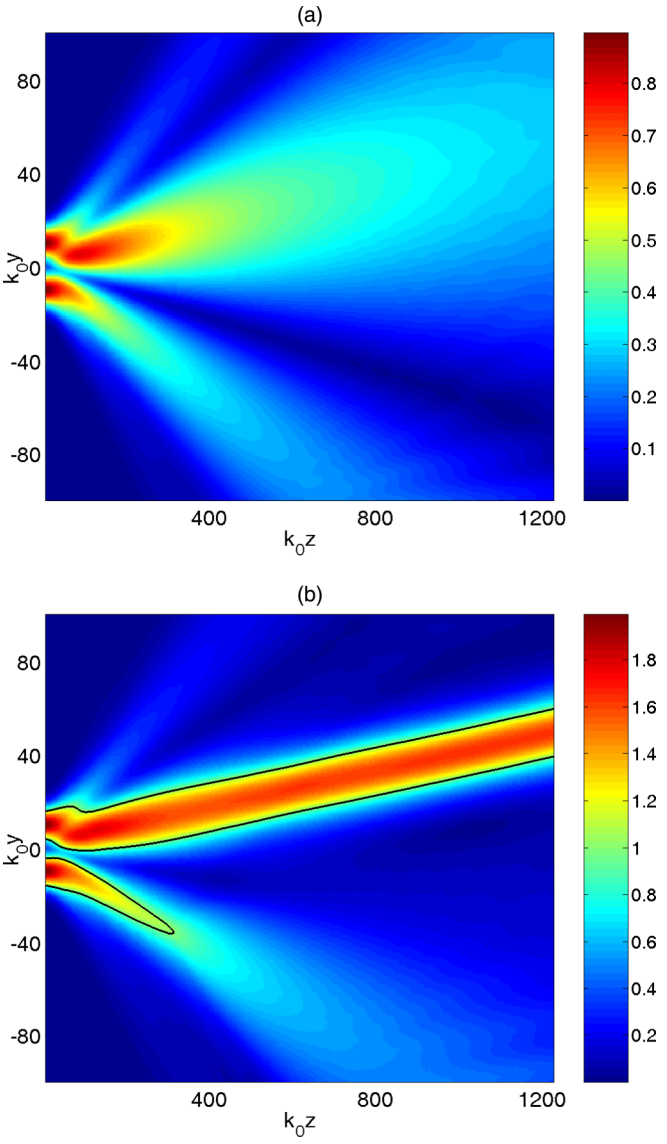

FIG. 7. (Color online) Spatial structure of normalized field $|E/E_c|$ in the case of subcritical (a) and supercritical (b) amplitude; the solid line shows the boundaries of the reoriented meta-atom domain. The field amplitude at $z = 0$ is taken in the form of two Gaussian beams with the $\pi/2$ phase shift $E/E_c = A_0\{\exp[-(y/w - h)^2/2] + \exp[-(y/w + h)^2/2 + i\pi/2]\}$ with $h = 2$; $k_0 w = 5$; $A_0 = 0.9$ and 2 for the subcritical and supercritical structures, respectively; and $\omega/\omega_s = 0.95$.

the threshold beam power necessary for soliton excitation can be easily managed just by changing the dc field strength. Besides, E_C depends strongly on the wave frequency. All of this enables us to obtain the nondiverging wave beams in LMC with parameters prescribed beforehand. Moreover, our numerical simulations show an easy way to control the soliton structure and the direction of propagation by means of phase-shifting.

At frequencies above the resonant value, the nonlinear correction $\Delta\varepsilon$ to the effective permittivity of LMC is negative, which, it might seem, enables the dark spatial soliton formation. However, one can show that there are no dark soliton solutions.

The above analysis and the numerical calculations do not take into account thermal off-orientation of meta-atoms, which can influence the conditions for soliton creation and propagation, especially in the case of weak electric fields. The thermal fluctuations result in random reorientation of the meta-atoms, and the critical field E_T can be estimated from the condition of equality of the thermal energy $k_B T$ and the induced electric energy of meta-atom $2\varepsilon_l a l^2 E_T^2$. If the amplitude of the electric field, no matter how static or high frequency it is, exceeds E_T, the thermal disordering does not prevent the meta-atom alignment. The estimations give for the considered parameters $E_T \sim 21/\sqrt{\varepsilon_l}$ V/cm. The bistability threshold for this minimal constant field of ordering and, hence, the threshold of soliton excitation corresponds approximately to the energy density flux $S \sim 3 \times 10^{-4}/\epsilon_e$ W/cm^2. With increasing the dc field, this threshold power also increases proportionally to the squared constant field strength.

It should be noted that the thermal effects may somehow smooth the jump of permittivity at the interface of the reoriented meta-atom domain. However, the soliton structure is robust with respect to these boundary perturbations if the fields are considerably stronger than E_T. It is interesting to note that the averaged ponderomotive forces acting on the meta-atoms in the electromagnetic field result in adiabatically slow compression of the particle density near the soliton core, which in turn can enhance the localization of the electromagnetic field. Thus, it may increase the propagation distance of the spatial soliton.

V. CONCLUSIONS

In conclusion, the conditions were found of the instability development of LMC in the field of electromagnetic waves propagating along the dc field, which leads to the meta-atom turnover. The meta-atom upset changes the effective refraction index of LMC, which creates the possibility for photon trapping into a self-consistent waveguide channel, or, in other words, a spatial soliton. The excitation, stability, and propagation features of the spatial soliton have been studied. The numerical results presented in this paper are obtained for the microsized meta-atoms and terahertz frequency domain. Apparently, one can expect that similar effects can take place in the arrays of elongated metal *nanoparticles* under the action of visible light or near-infrared radiation, when the resonant properties of nanoparticles are related to plasmonic resonances. In contrast to the terahertz meta-atoms, the plasmonic particles at optical frequencies have a significantly lower resonance quality factor than that considered above, which results in increase of the soliton excitation threshold because of the expansion of the bistability region.

ACKNOWLEDGMENTS

This research was supported in part by the RFBR Grant No. 14-02-00439 and the agreement of August 27, 2013 No. 02.B.49.21.0003 between the Ministry of Education and Science of the Russian Federation and Lobachevsky State University of Nizhni Novgorod.

[1] A. A. Zharov, A. A. Zharov, Jr., and N. A. Zharova, J. Opt. Soc. Am. B **31**, 559 (2014).
[2] D. R. Smith, W. J. Padilla, D. C. Vier, S. C. Nemat-Nasser, and S. Schultz, Phys. Rev. Lett. **84**, 4184 (2000).
[3] R. A. Shelby, D. R. Smith, and S. Schultz, Science **292**, 77 (2001).
[4] S. Linden, C. Enkrich, M. Wegener, T. Zhou, T. Kochny, and C. M. Soukoulis, Science **306**, 1351 (2004).
[5] G. Dolling, M. Wegener, C. M. Soukoulis, and S. Linden, Opt. Lett. **32**, 53 (2007).
[6] U. K. Chettiar, A. V. Kidishev, H. K. Yuan, W. Cai, S. Xiao, V. P. Drachev, and V. M. Shalaev, Opt. Lett. **32**, 1671 (2007).
[7] H. J. Lezec, J. A. Dionne, and H. A. Atwater, Science **316**, 430 (2007).
[8] A. A. Zharov, I. V. Shadrivov, and Y. S. Kivshar, Phys. Rev. Lett. **91**, 037401 (2003).
[9] A. Minovich, J. Farnell, D. N. Neshev, I. McKervacher, F. Karouta, J. Tian, D. A. Powell, I. V. Shadrivov, H. H. Tan, C. Jagadish, and Yu. S. Kivshar, Appl. Phys. Lett. **100**, 121113 (2012).
[10] W. L. Barnes, A. Dereux, and A. Ebbensen, Nature (London) **424**, 824 (2003).
[11] J. A. Fan, K. Bao, L. Sun, J. Bao, V. N. Manoharau, P. Nordlander, and F. Capasso, Nano Lett. **12**, 5381 (2012).
[12] A. Wiener, A. I. Fernandez-Dominguez, A. P. Horsfield, J. B. Pendry, and S. A. Maier, Nano Lett. **12**, 3308 (2012).
[13] A. Boltasseva and H. A. Atwater, Science **331**, 290 (2011).
[14] M. Lapine, I. V. Shadrivov, D. A. Powell, and Y. S. Kivshar, Nat. Mater. **11**, 30 (2012).
[15] M. Lapine, I. V. Shadrivov, D. A. Powell, and Yu. S. Kivshar, Sci. Rep. **1**, 138 (2011).
[16] E. Wang, T. P. White, and K. R. Catchpole, Opt. Express **20**, 13226 (2012).
[17] J. T. Shen, P. B. Catrysse, and S. Fan, Phys. Rev. Lett. **94**, 197401 (2005).
[18] A. N. Lagarkov and V. N. Kissel, Phys. Rev. Lett. **92**, 077401 (2004).
[19] N. Fang, H. Lee, C. Sun, and X. Zhang, Science **308**, 534 (2005).
[20] X. Zhang and Z. Liu, Nat. Mater. **7**, 435 (2008).
[21] D. K. Gramotnev and S. I. Bozhevolnyi, Nat. Photon. **4**, 83 (2010).
[22] V. M. Shalaev and S. Kawata, *Nanophotonics with Surface Plasmons* (Elsevier Science, Amsterdam, 2007).
[23] M. I. Stockman, Phys. Rev. Lett. **93**, 137404 (2004).
[24] A. R. Davoyan, I. V. Shadrivov, A. A. Zharov, D. K. Gramotnev, and Yu. S. Kivshar, Phys. Rev. Lett. **105**, 116804 (2010).
[25] D. J. Bergman and M. I. Stockman, Phys. Rev. Lett. **90**, 027402 (2003).
[26] I. Cao and M. L. Brongersma, Nat. Photon. **3**, 12 (2009).
[27] X. Meng, U. Guler, A. V. Kidishev, K. Fujita, K. Tanaka, and V. M. Shalaev, Sci. Rep. **3**, 1241 (2013).
[28] D. Schurig, J. J. Mock, B. J. Justice, S. A. Cummer, J. B. Pendry, A. F. Starr, and D. R. Smith, Science **314**, 977 (2006).

[29] B. Edwards, A. Alu, M. G. Silveirinha, and N. Engheta, Phys. Rev. Lett. **103**, 153901 (2009).

[30] N. A. Zharova, A. A. Zharov, and A. A. Zharov, Jr., Phys. Rev. A **89**, 043801 (2014).

[31] P. G. deGennes and J. Prost, *The Physics of Liquid Crystals*, 2nd paperback ed. (Clarendon, Oxford, 1995).

[32] R. Ramos-Garcia, I. Lazo-Martinez, I. Guizar-Iturbide, A. Sanchez-Castillo, M. Boffety, and P. Ruck, Mol. Cryst. Liq. Cryst. **454**, 179 (2006).

[33] J. S. Schwinger, L. L. Deraad, Jr., K. A. Milton, and W. Tsai, *Classical Electrodynamics* (Perseus Books, Reading, MA, 1998).

[34] M. Born and E. Wolf, *Principles of Optics*, 2nd (revised) ed. (Pergamon Press, London, 1964).

[35] N. G. Vakhitov and A. A. Kolokolov, Radiophys. Quantum Electron. **16**, 783 (1973).

[36] Y. S. Kivshar and G. P. Agrawal, *Optical Solitons. From Fibers to Photonic Crystals* (Academic Press, San Diego, 2003).